ACS OMEGA

Article

Cite This: ACS Omega 2019, 4, 22126−22132

http://pubs.acs.org/journal/acsodf

Octametallic Cluster of Cp*Ir(glycinato) Cations

David M. Morris and Joseph S. Merola*

Department of Chemistry, Virginia Tech, Blacksburg, Virginia 24061, United States

Supporting Information

ABSTRACT: Removal of chloride from Cp*Ir(glycinato)Cl in noncoordinating solvents with $Ag[PF_6]$ or $Tl[PF_6]$ leads to the formation of a closed octametallic loop of cations. The same loop also sequesters a number of PF_6^- counter anions. This is in contrast with reports that piano-stool complexes with amino acids form only trimetallic $[Cp^*Ir(aminoacidato)]_3^{3+}$ moieties upon creating the cation. Cp*Ir(glycinato)Cl also forms a trimetallic compound as well as a octametallic compound, and the octametallic vs trimetallic formation appears to be dependent on the anion. The synthesis and characterization of the octametallic complex, as well as some monometallic and trimetallic compounds, are reported, including the X-ray crystal structures.

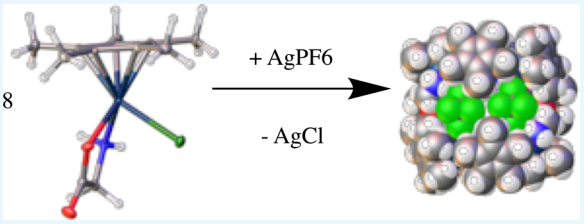

1. INTRODUCTION

There is a very rich chemistry of transition metals with amino acid ligands.[1−4] Within that large group, piano-stool complexes, especially of osmium, ruthenium, rhodium, and iridium, with amino acid ligands show a particular aptitude for self-assembly into polynuclear complexes. In the former two cases (Ru and Os), the "seat" of the piano stool is usually a neutral benzenoid ligand such as benzene, mesitylene, hexamethylbenzene or a host of other substituted benzenes.[5−7] For the latter two cases (Rh and Ir), the aromatic π ligand is most usually cyclopentadienide or a plethora of continually evolving substituted cyclopentadienides.[8−12] In both cases, with the anion of the amino acid, a neutral piano-stool complex of ruthenium(II), osmium(II), rhodium(III), and iridium(III) is formed with the third leg of the piano stool being a negatively charged ligand such as a halide or a pseudohalide. A halide can be removed using silver tetrafluoroborate, silver hexafluorophosphate, or a silver (or thallium) salt of other weakly coordinating anions. In a coordinating solvent, that solvent can replace the halide ion. In a noncoordinating solvent, there are several examples where a halide removal reaction leads to self-assembly yielding trinuclear piano-stool compounds. The assembly involves the amino acid moieties wherein the carboxylate of the amino acid bridges the metal centers.

In 2008, Alessio et al. wrote a detailed review of tri- and tetrametallic compounds formed from suitably bridging ligands and the bridge is not limited to amino acids by any means, but they do dominate. Whatever the potential linking ligand, the dominant motif appears to be the formation of what Alessio called "metallatriangles".[13] Beck et al. showed that a pentamethylcyclopentadienyl (Cp*) complex of Rh and phenylalanine can be induced to form metallotriangles by chloride removal with silver BF_4.[14] Carmona et al. reported the synthesis of four such trinuclear species beginning with (*p*-cymene)Os(amino acid)Cl complexes and silver tetrafluoroborate.[15] Many other types of bridging ligands have been used to create shapes such as metallarectangles[16] and other tetra-, hexa-, and dodecanuclear Ir compounds.[17] A recent review by Milios et al. focuses on the chemistry specifically for amino acids.[18] For piano-stool complexes of Ru, Os, Rh, and Ir, the trimetallic complexes with bridging amino acid ligands dominate.

In this paper, we report our findings in the area pioneered by Carmona and Beck, among others, that the formation of polymetallic compounds with bridging amino acids occurs on replacing a halide ligand with a poorly coordinating anion. For this specific area of amino acid half-sandwich compounds, the literature is relatively emphatic that only trinuclear compounds are formed. We here show that the nuclearity is not only limited to trinuclear species but also can form other species depending on the amino acid and the counterion. An unprecedented octametallic complex is described. We have been examining, in some detail, the bis acidato amine complexes of palladium as well as the acidato amine piano-stool complexes of $Cp^{*R}M$ where M = Rh, Ir, and Cp^{*R} refers to tetramethyl cyclopentadienide compounds where the 5th position is a group other than methyl.[19] We have published on the syntheses of many $Cp^{*R}Ir$ and Rh compounds previously.[20−23]

2. RESULTS AND DISCUSSION

2.1. Monometallic Complexes. *2.1.1. Neutral Piano-Stool Compounds.* The addition of amino acids to $[Cp^{*R}IrCl_2]_2$ yields piano-stool complexes of the form $Cp^{*R}M(aa)Cl$ (aa = amino acidato) complexes. In general, the most studied amino acid and the one that yields the most interesting catalytic asymmetric transformations is proline. We

Received: October 3, 2019
Accepted: November 28, 2019
Published: December 11, 2019

DOI: 10.1021/acsomega.9b03267
ACS Omega 2019, 4, 22126−22132

have reported previously on the combinations of Cp*R and azetidine, proline and pipecolic acid to yield asymmetric transfer hydrogenation (ATH) catalysts.[19] This paper will focus on Cp* only and on glycine and proline solely for the purpose of examining the self-assembly of cations formed upon chloride removal.

Addition of two equivalents of L-proline to $[Cp^{*R}IrCl_2]_2$ affords an excellent yield of Cp*Ir(L-prolinato)Cl, complex **1**. Characterization by NMR spectroscopy, high-resolution mass spectroscopy (HRMS), C, H analysis, and X-ray crystallography all confirm the composition. We have already reported on a number of Cp^{*R} iridium amino acid complexes,[19] and the crystal structure of complex **1** has been reported by Carmona et al.[10] There is a distinction to be made here concerning the diastereomers found in the solid state compared with what occurs in solution. We obtained a crystal structure of complex **1** to confirm it is the same as reported by Carmona as well as to have a low-temperature structure for a more direct comparison to our other compounds. For the figure and the experimental data for compound **1**, please see the Supporting information. The solution behavior of **1** is worth noting. When Cp*Ir(L-Pro)Cl from the reaction mixture is dissolved in $CDCl_3$ and the ^1H NMR spectrum obtained, there are signals for two isomers, presumably arising from the two diastereomers. In the single crystal, the ratio of the diastereomers is 50:50, but in solution, it is 92:8. A crystal was screened by X-ray diffraction to confirm that it was the same as that used to determine the single-crystal X-ray structure. That single crystal (with the 50:50 diastereomer ratio) was dissolved in $CDCl_3$, and the ^1H NMR spectrum shows that epimerization at the metal center is rapid, obtaining the same solution ratio as the bulk sample in a matter of seconds. Monitoring of the ^1H NMR spectrum over a period of several days shows no change in this ratio suggesting that this is the thermodynamic ratio of the two diastereomers. NOE experiments showed that, in solution, the major isomer is the one with the S configuration at the metal.

To probe this ratio further, density functional theory (DFT) calculations using the WebMO interface[24] to Gaussian 09[25] at the B3LYP level of theory[26,27] using the lanl2dz basis set[28] were carried out on the two diastereomers. The two diastereomers showed a ΔG difference of 15 kJ/mol in favor of the S configuration at the metal when using L-proline. This magnitude of ΔG suggests an equilibrium in favor of the S configuration at the metal with a S/R ratio of approximately 97/3. The actual solution ratio of 92/8 is in good agreement given that there is a solvent effect on this ratio that is not accounted for in the DFT experiments. The diastereomeric ratio is also consistent with what has been reported by others.[7]

The addition of 2 equivalents of glycine and base to $[Cp^*Ir(Cl)_2]_2$ produces complex **2**, Cp*Ir(glycinato)Cl, in good yield. Complex **2** has been synthesized previously and our characterization matches that from the literature, including the single-crystal X-ray structure.[29] Glycine is not a chiral amino acid; however, the presence of 4 different groups around the pseudo-tetrahedral iridium atom makes the iridium a chiral center. As is expected for enantiomers, both display identical NMR spectra, and both enantiomers are seen in the X-ray crystal structure (as well as a molecule of dichloromethane (DCM) of solvation). Again, we obtained the X-ray data for both to confirm the same structure as previously reported and to have low-temperature data (See the Supporting information).

2.1.2. Cationic Piano-Stool Compounds. Removal of a chloride ion from Cp*M(aa)Cl using a silver salt with a noncoordinating counterion works quite well with iridium piano-stool compounds to generate a cationic species. In the presence of a coordinating solvent, that solvent often will take the place of the lost chloride ion generating $[Cp^*Ir(aa)S]^+$ species (S = solvent). When Cp*Ir(glycinato)Cl was treated with $AgBF_4$ in acetonitrile, the cation [Cp*Ir(glycinato)-(acetonitrile)]$^+$, complex **3**, was formed. This salt was isolated and characterized by NMR spectroscopies, HRMS, and by single-crystal X-ray diffraction. The thermal ellipsoid plot of complex **3** is shown in Figure 1. Limbach et al. reported this

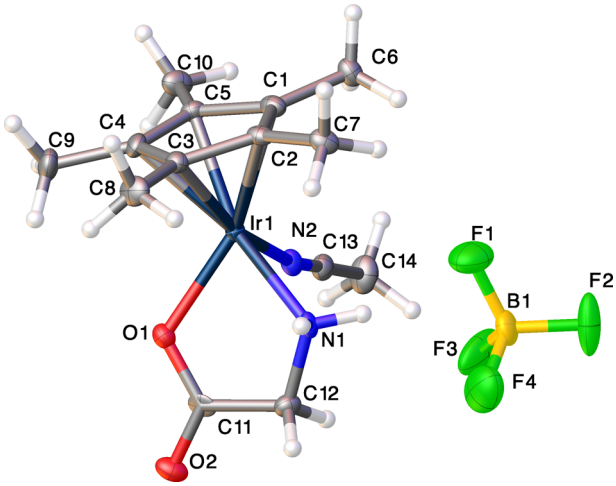

Figure 1. Thermal ellipsoid plot of [Cp*Ir(glycinato)(acetonitrile)]-[BF_4], complex **3**. Ellipsoids are shown at 50% probability.

cation as a triflate salt.[11] We obtained the crystal structure of **3** to confirm that the same trimetallic cluster was formed with different anions. The crystals of the BF_4^- salt described here are somewhat twinned and consist of a portion of both enantiomers. Refinement with the TWIN law in SHELX of -1 0 0 0 -1 0 0 0 -1 converged to a value of 0.28 for the Flack parameter indicating a 72/28 ratio of the enantiomers.

2.2. Polymetallic Complexes. Carmona *et al.* showed that removal of chloride with $AgBF_4$ from Cp*Ir(L-alaninato)Cl in methanol would yield a trimetallic, tricationic compound as the BF_4^- salt with R-configuration at iridium. The cation generated from Cp*Ir(L-alaninato)Cl has been isolated and structurally characterized by perchlorate[30] and triflate[14] counterions. While inclusion of solvent or the anion may differ, all cations show the same trinuclear arrangement with L-proline yielding the R-configuration at the metal. We used $AgPF_6$ to generate the cation and, while the structure has the disorder of the Cp* rings, it shows the same features: space group $P6_3$ and a trimetallic cluster with metal centers bridged by the carboxylate of the amine acidato group. The same motif holds true with other chiral amino acid cations such as valine. While we have formed several amino acid trimetallic clusters of Cp*Ir, only one, that of proline, yielded crystals suitable for X-ray diffraction (Figure 2).

When the nonchiral amino acid, glycine, is the ligand on the piano-stool compound, we find the same result of trimer formation when the halide reacts with $AgBF_4$. The BF_4^- salt crystallizes from *N*,*N*-dimethylformamide/hexanes in P$\bar{1}$ with the crystal lattice retaining four molecules of DMF and 0.5 molecules of cyclohexane (we assume that this was a small

DOI: 10.1021/acsomega.9b03267
ACS Omega 2019, 4, 22126−22132

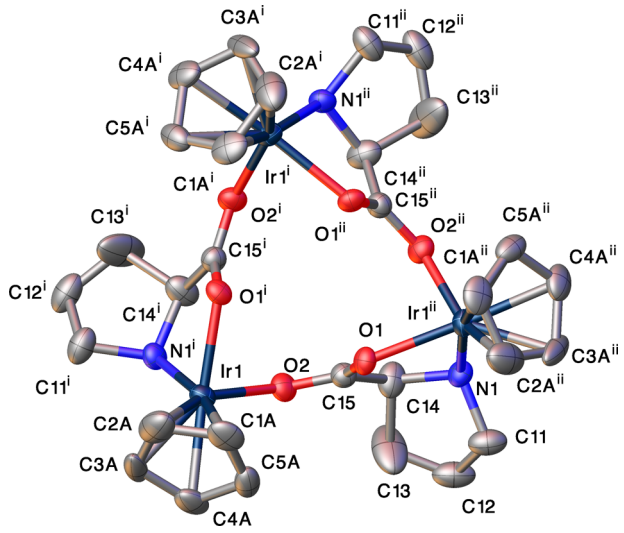

Figure 2. Thermal ellipsoid plot of $[Cp^*Ir(L\text{-prolinato})]_3[PF_6]_3$, complex **4**. Hydrogen atoms and Cp* methyl carbons eliminated for clarity. Only one part of the disordered Cp is shown. Ellipsoids are shown at 50% probability.

component of the hexanes mixture) per trimetallic unit. The geometry about each metal center is R, R, R (the glycine trimetallic cation has been reported previously by Limbach et al. with a triflate counterion. The trimetallic core appears to be the same with both BF_4^- and triflate (Figure 3).[11])

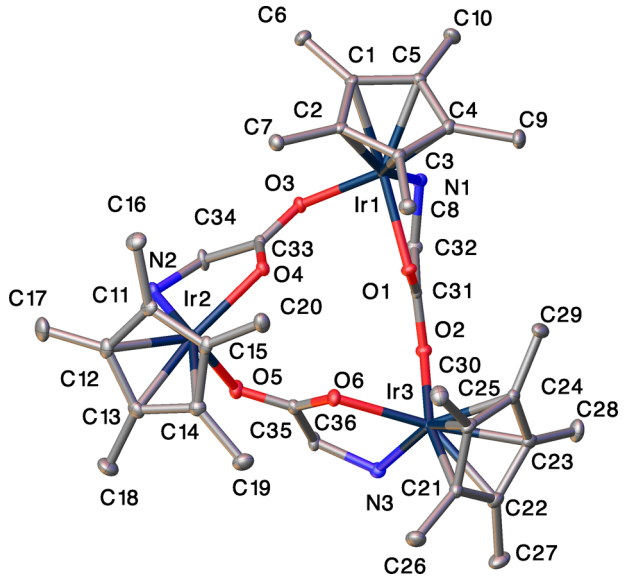

Figure 3. Thermal ellipsoid plot of $[Cp^*Ir(glycinato)]_3[BF_4]_3$, compound 5. Hydrogen atoms eliminated for clarity. Ellipsoids are shown at 50% probability.

However, when Cp*Ir(glycinato)Cl was treated with $TlPF_6$, a new and unprecedented octametallic cluster was formed, and the core of the cluster is shown in Figure 4. The octamer is formed with semialternating chiral units of the form $R_{Ir}R_{Ir}S_{Ir}S_{Ir}R_{Ir}R_{Ir}S_{Ir}S_{Ir}$. The asymmetric unit contains only half of the structure, with the octamer completed through a C_2 rotation. The Ir−O bond strengths differ slightly, even between enantiomers of the same configuration (see Table 1 for comparison of selected bond distances and angles of the

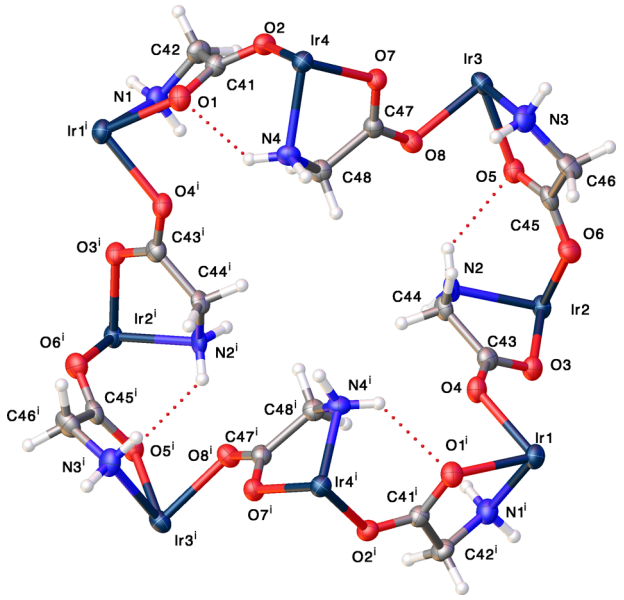

Figure 4. Thermal ellipsoid plot of the core of $[Cp^*Ir(glycinato)]_8[PF_6]_8$, complex **6**. Cp* groups are omitted for clarity. Ellipsoids are shown at 50% probability.

different enantiomers of the monometallic glycine complex, compound 2, and the four unique metal centers of the octametallic complex, compound 5. Also, see 4 for the numbering of the iridium units.) Units 1 and 4, both R_{Ir} have Ir−O bond lengths of 2.134(6) and 2.126(5) Å. Similarly, units 2 and 3 have lengths of 2.140(6) and 2.119(4) Å. Gly1 and Gly2 refer to the independent units in the monomeric Cp*RIr(Gly)Cl (compound 1). In general, the Ir−O distances are shorter in the monomeric complexes vs the octameric complex. The differences in bond lengths and angles are brought on by the constraints imparted by the ring system formed. In addition to the number of units in the structure, there are interesting features in the bonding. As can be seen in Figure 4, there are strong hydrogen-bonding interactions between one of the glycine N−H atoms and a nonbridging oxygen of an adjacent molecule. There are only 4 such N−H−O interactions around the torus, but there are other N−H hydrogen bond donor interactions with PF_6^- ions (as well as C−H−F interactions). The combination of these interactions gives an overall shape of a "crushed" or "bent" torus. A space-filling model of this shape viewed down what is a C_2 axis for the whole cluster can be found in Figure 5 and a side view in Figure 6. Both Figure 5 and especially Figure 6 show the large hole in the torus of the assembled cations.

The only difference between the formation of the trimetallic glycinato cluster complex **5** and the octametallic cluster **6** is the counteranion: BF_4^- vs PF_6^-. A closer view of both the anions and cations in the crystal lattice of $[Cp^*Ir(glycinato)]_8[PF_6]_8$ shows that the PF_6^- appears to play a critical role in the formation of the overall structure. Again, the structure of the assembled cations is a crushed torus with a C_2 axis and two pockets on either side of the octametallic complex. In each of those pockets, two PF_6^- ions sit, and the combination of the octametallic octacation and four of the PF_6^- counterions makes a solid molecular sphere (see Figures 7 and 8). When viewed at full van der Waals radii, the two PF_6^- ions in each pocket are held very closely together. The four additional PF_6^-

DOI: 10.1021/acsomega.9b03267
ACS Omega 2019, 4, 22126−22132

Table 1. Selected Bond Lengths (Å) and Angles (deg) of Glycine (Cp*)Ir(aa)Cl Complexes Gly1, Gly2 Refer to the Enantiomers of Compound 2 and 1[a]-4[a] Refer to the 4 Unique Iridium Centers in Compound 5

bond distance or angle	Gly1	Gly2	1[a]	2[a]	3[a]	4[a]
Ir−O(cord)	2.099(5)	2.108(2)	2.134(6)	2.140(6)	2.119(4)	2.126(5)
Ir−O(bridge)	n/a	n/a	2.138(5)	2.122(5)	2.134(5)	2.119(5)
Ir−N1	2.139(7)	2.111(7)	2.140(5)	2.146(7)	2.148(8)	2.130(7)
Ir−Cp*(centroid)	1.755	1.75	1.751	1.768	1.759	1.761
O(cord)−Ir−O(bridge)	n/a	n/a	79.0(2)	78.0(2)	78.0(2)	77.9(2)
O(cord)−Ir−N	78.31(9)	78.45(9)	77.5(2)	76.9(2)	77.6(2)	77.1(2)
O(bridge)−Ir−N	n/a	n/a	84.8(2)	81.7(2)	84.4(2)	81.1(2)
Cp*(centroid)−Ir−O(cord)	128.68	129.99	131.66	1311.09	132.02	129.94
Cp*(centroid)−Ir−O(bridge)	n/a	n/a	130.14	133.62	132.2	133.43
Cp*(centroid)−Ir−N	134.87	134.42	130.14	133.54	131.81	135.05

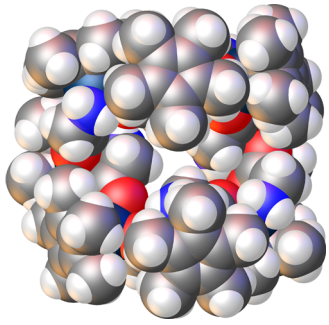

Figure 5. Space-filling plot of $[Cp^*Ir(glycinato)]_8^{8+}$ viewed down the C_2 axis of the torus. Atom radii are shown at full van der Waals' (VDW) values.

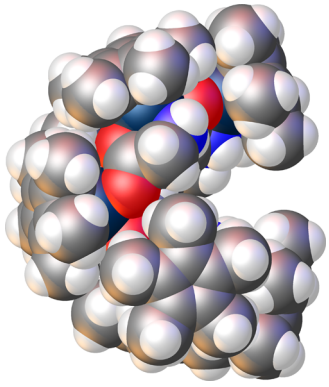

Figure 6. Space-filling plot of $[Cp^*Ir(glycinato)]_8^{8+}$ viewed from the side. Atom radii are shown at full van der Waals' values.

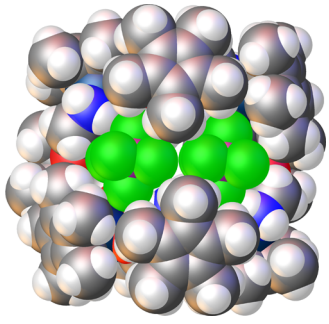

Figure 7. Space-filling plot of $[Cp^*Ir(glycinato)]_8^{8+}$ viewed along the C_2 axis showing inclusion of two of the PF_6^- counterions in a pocket of the torus. Atom radii are shown at full van der Waals' values.

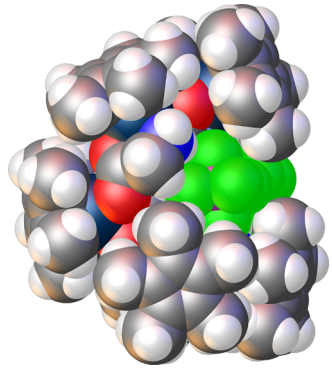

Figure 8. Space-filling plot of $[Cp^*Ir(glycinato)]_8^{8+}$ viewed from the side showing inclusion of PF_6^- ions in a pocket of the torus. Atom radii are shown at full van der Waals' values.

ions needed for neutrality are hydrogen-bonded to the "outside" of the molecular ball.

A calculation of close contacts (sum of VDW radii) between the PF_6^- and the backbone of the octamer reveals over 15 close contacts between the PF_6^- and N−H, C−H, and a number of other sites surrounding the pocket in which the PF_6^- ion is held. Examining stronger, closer contacts based on the sum of the VDW radii minus 0.2 Å shows that there are 6 particularly close (and presumably stronger) contacts for each PF_6^- ion: one NH···F contact of 2.439 Å, two C−H···F interactions of 2.46 Å to Cp* methyl groups, one C−H···F contact of 2.387 Å to a glycine C−H bond, and one C···F contact between a fluorine and the carboxylato carbon atom of a glycine ligand. With the exception of the NH···F hydrogen bond, none of the remaining interactions is what one would normally expect to be good anion binders, see Figure 9.

The way in which the PF_6^- ions are cradled in the octametallic complex is unique. As we (BF_4^-) and Rominger (triflate) have shown, both BF_4^- and triflate only form trimetallic compounds. Figure 10 depicts a space-filling plot of the glycine trimetallic, which clearly shows that there is no "hole" in the center of the trimetallic and while there are close contacts between the anions and the trimetallic, they are not "encapsulated" in the cation. So, we conclude that the interactions with PF_6^- are what drives the formation of the octametallic cation. Yu et al. reported triflate- and nitrate-induced self-assembly of ruthenium half-sandwich compounds of substituted 8-hydroxyquinoline ligands.[31] The phenomenon of anions inducing a particular supramolecular structure is known in other systems. Several reviews have been written about the influence of anions on supramolecular complexes,

DOI: 10.1021/acsomega.9b03267
ACS Omega 2019, 4, 22126−22132

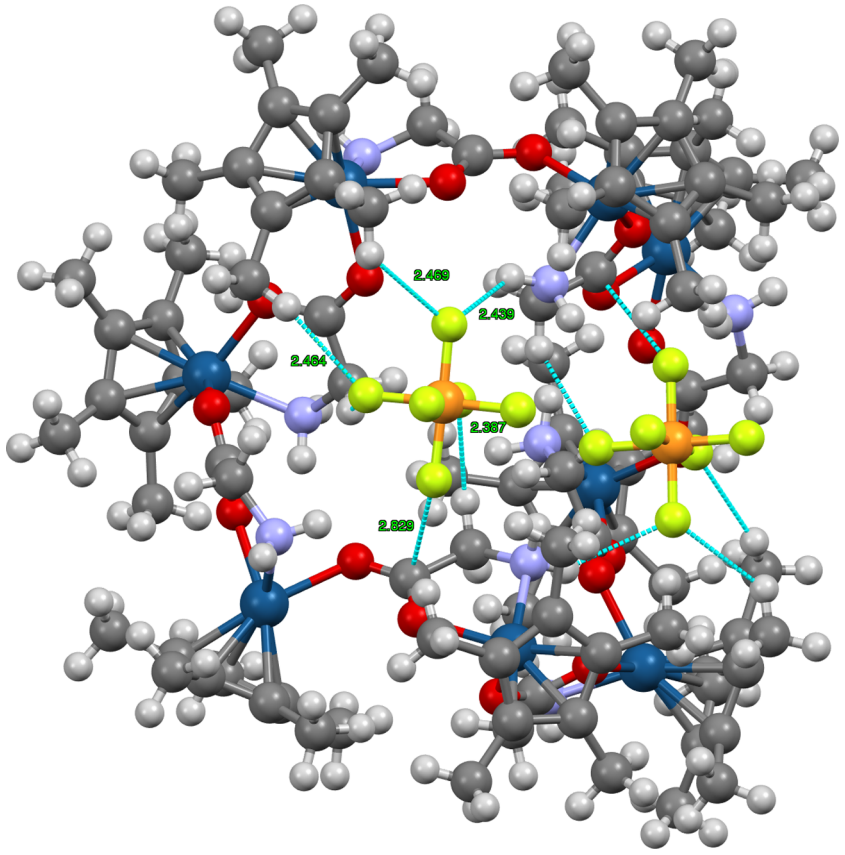

Figure 9. View of two of the encapsulated PF_6^- ions with short contacts indicated by blue dashed lines. The contact distances are shown in green and both PF_6^- ions have the same distances since they are related by symmetry.

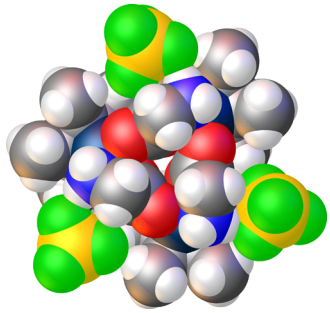

Figure 10. Space-filling model of the glycine trimetallic with the BF_4^- anions showing close contacts.

but the anion most often influences with π−anion interactions with other triggers causing a fully enclosed cavity to enclose the anion.[32−34] Multiple reviews of piano-stool complexes especially with amino-acid-type ligands with both Cp and arene ligands show that the trimetallic is formed no matter the anion.[13] The octametallic reported herein clearly shows a new mode of anion influence not seen before.

3. CONCLUSIONS

Investigations into the properties of piano-stool complexes of iridium and amino acids continue to unearth new discoveries of the bonding and self-assembly features of these moieties. We have created a significant library of Cp^{*R} with R ranging from H to linear alkyls with lengths as high as 12, branched alkyls, aryls, and aralkyl. The combinatorial possibilities for how the R group, the metal (Rh and Ir), and the amino acid affect the self-assembly are a continuing interest, but at the time of submitting this publication, many different combinations have been tried with no success. In this paper, we demonstrate that proline, as is the case with many reports of other amino acid complexes of Cp*Ir compounds, shows trimetallic cluster formation even with PF_6^- counterions but glycine shows a quite different behavior of forming the unique octametallic assembly. Future combinations will be investigated.

4. EXPERIMENTAL SECTION

4.1. General. All materials for synthesis, purification, and characterization were used as received unless otherwise stated. $IrCl_3 \cdot xH_2O$ was purchased from Pressure Chemical, Pittsburgh, PA 15201. L-Proline, D-proline, and pentamethylcyclopentadiene were purchased from Alfa Aesar, Ward Hill, MA 01835. $AgBF_4$, $AgPF_6$, $Tl[PF_6]$, and reagent grade solvents were purchased from Sigma-Aldrich, St. Louis, MO 63103. Glycine was purchased from Qiagen Sciences, Germantown, MD 20874. Deuterated solvents for NMR spectroscopy were obtained from Cambridge Isotope Laboratories, Tewksbury, MA 01876. $[Cp^{*R}IrCl_2]_2$ was synthesized as previously described.

Elemental analyses were performed by Atlantic Microlabs, Norcross, GA. ^1H NMR spectra were collected on a Varian MR-400 NMR spectrometer.

Mass spectrometry was performed by William Bebout of the Virginia Tech Chemistry Department Analytical Service laboratory in Blacksburg, VA. Positive ion electrospray ionization mass spectra ((+)ESI-MS)122 were collected using Agilent Technologies 6220 Accurate-Mass time-of-flight

DOI: 10.1021/acsomega.9b03267
ACS Omega 2019, 4, 22126−22132

(TOF) liquid chromatography−mass spectrometry (LC−MS) with a dual ESI source. The sample was dissolved in HPLC grade solvent and injected through a preloading capillary at 1.2 kV with a flow rate of 0.4 mL/min. N2 gas was used as the inert nebulizing gas at a pressure of 60 psig. The charging voltage was set to 2000 V, the fragmentor voltage set to 125 V, and the skimmer voltage set to 65 V.

X-ray crystallographic data were collected at 100 K on an Oxford Diffraction Gemini diffractometer with an EOS CCD detector and Mo Kα radiation. Crystals were coated in Paratone oil and mounted on a fiber. Data collection and data reduction were performed using Agilent's CrysAlisPro software.[35] Structure solution and refinement were performed with ShelXS[36] and SHELXL,[37] and Olex2 was used for graphical representation of the data.[38]

4.2. Syntheses. General procedure: An appropriately sized round-bottom flask was charged with required amounts of $[Cp^*IrCl_2]_2$, amino acid, base (KOH or $NaHCO_3$), and methanol. With magnetic stirring, the initial orange solution changed to yellow over the course of 30 min to 2 h depending on the amino acid used. The solvent was removed via reduced pressure. The complex was extracted with 3 × 10 mL of dichloromethane (DCM) and filtered to remove excess amino acid and base. The complexes were recrystallized by first dissolving the complexes in minimal DCM, followed by slow addition of either ether or hexanes to produce a yellow powder. The complexes were then collected on a frit as yellow crystalline powders.

*4.2.1. Synthesis of Cp*Ir(Gly)Cl.* Following the general procedure: $[Cp^*IrCl_2]_2$ (0.150 g, 0.189 mmol), glycine (0.058 g, 0.773 mmol), and KOH (0.043 g, 0.766 mmol) were reacted in methanol (25 mL) to give Cp*Ir(Gly)Cl (0.131 g, 0.300 mmol, 80%): ^{1}H NMR (400 MHz, $CDCl_3$) δ 6.49 (br s, 2H, NH_2), 3.45 (d, J = 6.0 Hz, 2H) CH_2, 1.71 (s, 15H, Cp*Me). ^{13}C NMR (101 MHz, $CDCl_3$) δ 183.4 (COO), 84.1 (Cp*), 45.3 (CH_2), 9.2 (Cp*Me). Single crystals suitable for X-ray diffraction were grown by slow diffusion of ether into DCM. HRMS/ESI+ (m/z): $[M + H]^+$ calcd for $C_{12}H_{19}NO_2[^{193}Ir$ 402.104; found, 402.1059. Anal Calcd for $C_{12}H_{19}ClIrNO_2.H_2O$: C, 31.68%; H, 4.65%. Found: C, 31.64%; H, 4.45%.

4.2.2. Synthesis of (Cp)Ir(L-Pro)Cl.* Following the general procedure: $[Cp^*IrCl_2]_2$ (0.100 g, 0.126 mmol), L-proline (0.0434 g, 0.377 mmol), and KOH (0.0211g, 0.377 mmol) were reacted in methanol (30 mL) to give (Cp*)Ir(L-Pro)Cl (0.107g, 0.224 mmol, 89%) (mol ratio of diastereomers 93/7, S/R): Major Isomer: ^{1}H NMR (400 MHz, $CDCl_3$) δ 4.64 (br s, 1H, NH), 4.12−4.00 (m, 1H, CHOO), 3.64−3.53 (m, 1H, NCH), 3.02−2.88 (m, 1H, NCH), 2.31−2.19 (m, 1H, CHH), 2.11−2.00 (m, 1H, CHH), 1.98−1.87 (m, 1H, CHH), 1.78−1.71 (m, 1H, CHH), 1.67 (s, 15H Cp*Me). ^{13}C NMR (101 MHz, $CDCl_3$) δ 184.2 (COO), 84.2 (Cp*), 62.4 (αCH), 54.7 (CH_2), 28.7 (CH2), 27.1 (CH_2), 9.2 (Cp*Me). Minor Isomer: ^{1}H NMR (400 MHz, $CDCl_3$) δ 6.73 (br s, 1H, NH), 4.25−4.18 (m, 1H, CHOO), 3.80−3.66 (m, 1H, NCH), 3.42−3.29 (m, 1H, NCH), 3.27−3.21 (m, 1H, CH), 2.11−1.99 (m, 2H, CH_2), 1.70 (s, 15H, Cp*Me). ^{13}C NMR (101 MHz, $CDCl_3$) δ 9.0 (CpMe). Single crystals suitable for X-ray diffraction were grown from slow diffusion of hexanes into dichloromethane HRMS/ESI+ (m/z): [M + H]+ calcd for $C_{15}H_{24}Cl[^{193}Ir]NO_2$ 478.1119; found 478.113. Anal. Calcd for $C_{15}H_{23}ClIrNO_2$: C, 37.77%; H, 4.86%. Found: C, 37.79%; H, 5.06%.

*4.2.3. Synthesis of [Cp*Ir(Gly)]$_8$[PF6]$_8$.* To a 50 mL round-bottom flask, 0.050 g (0.114 mmol) of [(Cp*)Ir(Gly)Cl] was added and dissolved in 20 mL of water. Thallium hexafluorophospate (0.042 g, 0.12 mmol) was added. The solution was stirred, and a white precipitate formed over the course of 30 min. Solvent was removed in vacuo, and the product was extracted with DCM and filtered. The octamer was recrystallized from DCM and hexanes to yield a yellow powder (0.362 g, 58%): ^{1}H NMR (400 MHz, CD_3OD) δ 5.64−5.52 (m, 1H, NH), 5.41−5.27 (m, 1H, NH), 3.85−3.71 (m, 1H, CHH), 3.27−3.19 (m, 1H, CHH), 1.74 (s, 15H, Cp*Me). ^{13}C NMR (101 MHz, CD_3OD) δ 189.0 (CHOO), 84.3 (Cp*), 45.0 (αC), 8.3 (Cp*Me). HRMS/ESI+ (m/z): calcd for $C_{12}H_{19}NO_2[^{193}Ir]$ 402.1045; found 402.0960. Anal. Calcd for $C_{96}H_{152}F_{48}Ir_8N_8O_{16}P_8$. 2($C_6H_{14}$); C, 28.55%; H, 3.99%; Found: C, 29.19%; H, 3.91%.

■ ASSOCIATED CONTENT

Supporting Information

The Supporting Information is available free of charge at https://pubs.acs.org/doi/10.1021/acsomega.9b03267.

Data from Gaussian calculations as well as full experimental details and crystallographic tables for the crystal structures numbered in this paper (PDF)

crystallographic data (CIF)

Accession Codes

CCDC 1947610-1947614 and 1013069 contain the supplementary crystallographic data for this paper. These data can be obtained free of charge via www.ccdc.cam.ac.uk/data_request/cif or by e-mail: data_request@ccdc.cam.ac.uk or by contacting The Cambridge Crystallographic Data Centre, 12 Union Road, Cambridge CB2 1EZ, U.K.; fax: +44 1223 336033.

■ AUTHOR INFORMATION

Corresponding Author

*E-mail: jmerola@vt.edu. Phone: +1 540 231-4510. Fax: +1 540 231-3255

ORCID

Joseph S. Merola: 0000-0002-1743-1777

Notes

The authors declare no competing financial interest.

■ ACKNOWLEDGMENTS

The authors thank Dr. Loren Brown and Dr. Christine DuChane for helpful discussions and work on some of the compounds discussed in this paper and Dr. Carla Slebodnick for help with the disordered proline trimer structure.

■ REFERENCES

(1) Jaouen, G.; Vessiéres, A.; Butler, I. S. Bioorganometallic Chemistry: A Future Direction for Transition Metal Organometallic Chemistry? *Acc. Chem. Res.* **1993**, *26*, 361−369.

(2) Jaouen, G.; Beck, W.; McGlinchey, M. J. A Novel Field of Research: Bioorganometallic Chemistry, Origins, and Founding Principles. 2005, https://doi.org/10.1002/3527607692.ch1.

(3) Jaouen, G.; Beck, W.; McGlinchey, M. J.. In *Bioorganometallics*, Jaouen, G., Ed.; Wiley-VCH Verlag GmbH & Co. KGaA: Weinheim, FRG, 2006; pp 1−37.

(4) Fish, R. H.; Jaouen, G. Bioorganometallic chemistry: Structural diversity of organometallic complexes with bioligands and molecular recognition studies of several supramolecular hosts with biomolecules,

DOI: 10.1021/acsomega.9b03267
ACS Omega 2019, 4, 22126−22132

alkali-metal ions, and organometallic pharmaceuticals. *Organometallics* **2003**, *22*, 2166−2177.
(5) Singh, A. K.; Pandey, D. S.; Xu, Q.; Braunstein, P. Recent advances in supramolecular and biological aspects of arene ruthenium(II) complexes. *Coord. Chem. Rev.* **2014**, *270-271*, 31−56.
(6) Therrien, B. The Role of the Second Coordination Sphere in the Biological Activity of Arene Ruthenium Metalla-Assemblies. *Front. Chem.* **2018**, *6*, No. 602.
(7) Carmona, D.; Lamata, M. P.; Oro, L. A. Half-sandwich complexes with aminocarboxylate ligands and their use as enantioselective hydrogen transfer catalysts. *Eur. J. Inorg. Chem.* **2002**, 2239−2251.
(8) Grotjahn, D. B.; Groy, T. L. Formation and Structure of Coordinatively Unsaturated Cp*Ir-Amino Acid Complexes. Kinetic and Thermodynamic Control in Highly Diastereoselective Complexation Reactions. *Organometallics* **1995**, *14*, 3669−3682.
(9) Carmona, D.; Vega, C.; Lahoz, F. J.; Atencio, R.; Oro, L. A.; Lamata, M. P.; Viguri, F.; San José, E. Synthesis and stereochemistry of half-sandwich alkynyl amino acidate complexes of rhodium(III), iridium(III), and ruthenium(II). *Organometallics* **2000**, *19*, 2273−2280.
(10) Carmona, D.; Pilar Lamata, M.; Viguri, F.; San José, E.; Mendoza, A.; Lahoz, F. J.; García-Orduña, P.; Atencio, R.; Oro, L. A. Half-sandwich organometallic complexes with stereogenic metal centres: Synthesis and characterization of diastereomeric [(η-ring)M(Aa)X] (Aa = α-amino carboxylate) compounds. *J. Organomet. Chem.* **2012**, *717*, 152−163.
(11) Wöckel, S.; Plessow, P.; Schelwies, M.; Brinks, M. K.; Rominger, F.; Hofmann, P.; Limbach, M. Alcohol amination with aminoacidato Cp*Ir(III)-complexes as catalysts: Dissociation of the chelating ligand during initiation. *ACS Catal.* **2014**, *4*, 152−161.
(12) Biancalana, L.; Abdalghani, I.; Chiellini, F.; Zacchini, S.; Pampaloni, G.; Crucianelli, M.; Marchetti, F. Ruthenium Arene Complexes with α-Aminoacidato Ligands: New Insights into Transfer Hydrogenation Reactions and Cytotoxic Behaviour. *Eur. J. Inorg. Chem.* **2018**, *2018*, 3041−3057.
(13) Zangrando, E.; Casanova, M.; Alessio, E. Trinuclear metallacycles: Metallatriangles and much more. *Chem. Rev.* **2008**, *108*, 4979−5013.
(14) Sünkel, K.; Hoffmüller, W.; Beck, W. Metal Complexes of Biologically Important Ligands, CVII [1], Formation of Tris-(pentamethylcyclopentadienyl-μ-L-prolinato-iridium) Tris-(trifluoromethanesulfonate) with Chiral Self Recognition. *Z. Naturforsch. B* **1998**, *53*, 1365−1368.
(15) Carmona, D.; Lahoz, F. J.; Atencio, R.; Oro, L. A.; Lamata, M. P.; Viguri, F.; San José, E.; Vega, C.; Reyes, J.; Joó, F.; Kathó, Á. Trimerisation of the Cationic Fragments [(η-ring)M(Aa)]+ ((η-ring)M=(η5-(C_5Me_5)Rh, (η5-(C_5Me_5)Ir, (η6-p-(MeC_6H_4iPr)Ru; Aa=α-amino acidate) with Chiral Self-Recognition: Synthesis, Characterisation, Solution Studies and Catalytic Reactions of the Trimers [(η-ring)M(Aa)$_3$(BF_4)$_3$. *Chem. - Eur. J.* **1999**, *5*, 1544−1564.
(16) Orhan, E.; Garci, A.; Therrien, B. Coordination-driven self-assembly of arene ruthenium metalla-rectangles. *Inorg. Chim. Acta* **2017**, *461*, 78−83.
(17) Lee, S. G.; Ryu, J. Y.; Stang, P. J.; Lee, J. Tetra-, Hexa-, Dodeca-Nuclear Ir Supramolecules via Bridge-Driven Self-Assembly of Tetrazolyl Ligands. *Inorg. Chem.* **2018**, *57*, 8054−8057.
(18) Canaj, A. B.; Kakaroni, F.; Collet, A.; Milios, C. J. α-Amino acids: Natural and artificial building blocks for discrete polymetallic clusters. *Polyhedron* **2018**, *151*, 1−32.
(19) Morris, D. M.; McGeagh, M.; De Peña, D.; Merola, J. S. Extending the range of pentasubstituted cyclopentadienyl compounds: The synthesis of a series of tetramethyl(alkyl or aryl)-cyclopentadienes (Cp*R), their iridium complexes and their catalytic activity for asymmetric transfer hydrogenation. *Polyhedron* **2014**, *84*, 120−135.
(20) Karpin, G. W.; Merola, J. S.; Falkinham, J. O. Transition Metal-α-Amino Acid Complexes with Antibiotic Activity against Mycobacterium spp. *Antimicrob. Agents Chemother.* **2013**, *57*, 3434−3436.
(21) Brown, L. C.; Ressegue, E.; Merola, J. S. Rapid Access to Derivatized, Dimeric, Ring-Substituted Dichloro(cyclopentadienyl)-rhodium(III) and Iridium(III) Complexes. *Organometallics* **2016**, *35*, 4014−4022.
(22) DuChane, C. M.; Brown, L. C.; Dozier, V. S.; Merola, J. S. Synthesis, Characterization, and Antimicrobial Activity of RhIII and IrIII β-Diketonato Piano-Stool Compounds. *Organometallics* **2018**, *37*, 530−538.
(23) DuChane, C. M.; Karpin, G. W.; Ehrich, M.; Falkinham, J. O.; Merola, J. S. Iridium piano stool complexes with activity against S. aureus and MRSA: it is past time to truly think outside of the box. *Medchemcomm* **2019**, *10*, 1391−1398.
(24) Schmidt, J.; Polik, W. WebMO Enterprise. https://www.webmo.net/.
(25) Frisch, M. J.. et al.*Gaussian 09*; Gaussian Inc.: Wallingford, CT, 2016.
(26) Becke, A. D. Density-functional thermochemistry. III. The role of exact exchange. *J. Chem. Phys.* **1993**, *98*, 5648−5652.
(27) Lee, C.; Yang, W.; Parr, R. G. Development of the Colle-Salvetti correlation-energy formula into a functional of the electron density. *Phys. Rev. B* **1988**, *37*, 785−789.
(28) Hay, P. J.; Wadt, W. R. Ab initio effective core potentials for molecular calculations. Potentials for K to Au including the outermost core orbitals. *J. Chem. Phys.* **1985**, *82*, 299−310.
(29) Wetzel, A.; Wöckel, S.; Schelwies, M.; Brinks, M. K.; Rominger, F.; Hofmann, P.; Limbach, M. Selective alkylation of amines with alcohols by Cp*- iridium(III) half-sandwich complexes. *Org. Lett.* **2013**, *15*, 266−269.
(30) Poth, T.; Paulus, H.; Elias, H.; Dücker-Benfer, C.; van Eldik, R. Kinetics and Mechanism of Water Substitution at Half-Sandwich Iridium(III) Aqua Cations Cp*Ir(A-B)(H_2O)$_2^+$ in Aqueous Solution (Cp* = η5-Pentamethylcyclopentadienyl Anion; A-B = Bidentate N,N or N,O Ligand). *Eur. J. Inorg. Chem.* **2001**, *2001*, 1361−1369.
(31) Yu, W. B.; He, Q. Y.; Shi, H. T.; Yuan, G.; Wei, X. Anion-directed self-assembly of two half-sandwich ruthenium-based metallamacrocycles as catalysts for water oxidation. *Chem.− Asian J.* **2015**, *10*, 239−246.
(32) Chifotides, H. T.; Dunbar, K. R. Anion-π interactions in supramolecular architectures. *Acc. Chem. Res.* **2013**, *46*, 894−906.
(33) Custelcean, R. Anion encapsulation and dynamics in self-assembled coordination cages. *Chem. Soc. Rev.* **2014**, *43*, 1813−1824.
(34) Juwarker, H.; Jeong, K. S. Anion-controlled foldamers. *Chem. Soc. Rev.* **2010**, *39*, 3664−3674.
(35) *CrysAlisPRO*; Oxford Diffraction/Agilent Technologies UK Ltd: Yarnton, England.
(36) Sheldrick, G. M. A short history of *SHELX*. *Acta Crystallogr., Sect. A: Found. Crystallogr.* **2008**, *64*, 112−122.
(37) Sheldrick, G. M. Crystal structure refinement with *SHELXL*. *Acta Crystallogr., Sect. C: Struct. Chem.* **2015**, *71*, 3−8.
(38) Dolomanov, O. V.; Bourhis, L. J.; Gildea, R. J.; Howard, J. A. K.; Puschmann, H. IUCr, *OLEX2*: a complete structure solution, refinement and analysis program. *J. Appl. Crystallogr.* **2009**, *42*, 339−341.

DOI: 10.1021/acsomega.9b03267
ACS Omega 2019, 4, 22126−22132